THE JOURNAL OF BIOLOGICAL CHEMISTRY VOL. 288, NO. 41, pp. 29333–29344, October 11, 2013

Lack of CD47 Impairs Bone Cell Differentiation and Results in an Osteopenic Phenotype *in Vivo* due to Impaired Signal Regulatory Protein α (SIRPα) Signaling*

Received for publication, June 18, 2013, and in revised form, August 14, 2013 Published, JBC Papers in Press, August 29, 2013, DOI 10.1074/jbc.M113.494591

Cecilia Koskinen[‡], Emelie Persson[‡], Paul Baldock[§], Åsa Stenberg[¶], Ingrid Boström[‡], Takashi Matozaki[‖], Per-Arne Oldenborg[¶], and Pernilla Lundberg[‡1]

From the Departments of [‡]Odontology, Section for Molecular Periodontology, Umeå University, 901 87 Umea, Sweden, the [§]Neurological Diseases Division, Garvan Institute of Medical Research, Darlinghurst, New South Wales 2010, Australia, [¶]Integrative Medical Biology, Section for Histology and Cell Biology, Umeå University, 901 87 Umea, Sweden, and the [‖]Department of Biochemistry and Molecular Biology, Division of Molecular and Cellular Signaling, Kobe University Graduate School of Medicine, Kobe 650-0017, Japan

Background: CD47 and its receptor SIRPα are suggested to regulate bone metabolism.
Results: Lack of CD47 prevents stromal cell SIRPα signaling, which impairs bone marrow stromal cell differentiation, subsequent osteoclast differentiation, and bone homeostasis.
Conclusion: CD47 and SIRPα both mediate normal bone cell and bone tissue formation.
Significance: CD47/SIRPα may be a future molecular target to modulate bone homeostasis.

Here, we investigated whether the cell surface glycoprotein CD47 was required for normal formation of osteoblasts and osteoclasts and to maintain normal bone formation activity *in vitro* and *in vivo*. In parathyroid hormone or 1α,25(OH)$_2$-vitamin D3 (D3)-stimulated bone marrow cultures (BMC) from *CD47*$^{-/-}$ mice, we found a strongly reduced formation of multinuclear tartrate-resistant acid phosphatase (TRAP)$^+$ osteoclasts, associated with reduced expression of osteoclastogenic genes (*nfatc1*, *Oscar*, *Trap/Acp*, *ctr*, *catK*, and *dc-stamp*). The production of M-CSF and RANKL (receptor activator of nuclear factor κβ ligand) was reduced in *CD47*$^{-/-}$ BMC, as compared with *CD47*$^{+/+}$ BMC. The stromal cell phenotype in *CD47*$^{-/-}$ BMC involved a blunted expression of the osteoblast-associated genes osterix, *Alp*/*Akp1*, and α-1-collagen, and reduced mineral deposition, as compared with that in *CD47*$^{+/+}$ BMC. CD47 is a ligand for SIRPα (signal regulatory protein α), which showed strongly reduced tyrosine phosphorylation in *CD47*$^{-/-}$ bone marrow stromal cells. In addition, stromal cells lacking the signaling SIRPα cytoplasmic domain also had a defect in osteogenic differentiation, and both *CD47*$^{-/-}$ and non-signaling SIRPα mutant stromal cells showed a markedly reduced ability to support osteoclastogenesis in wild-type bone marrow macrophages, demonstrating that CD47-induced SIRPα signaling is critical for stromal cell support of osteoclast formation. *In vivo*, femoral bones of 18- or 28-week-old *CD47*$^{-/-}$ mice showed significantly reduced osteoclast and osteoblast numbers and exhibited an osteopenic bone phenotype. In conclusion, lack of CD47 strongly impairs SIRPα-dependent osteoblast differentiation, deteriorate bone formation, and cause reduced formation of osteoclasts.

Resorption of bone is essential for the regeneration of the adult skeleton. After growth, old bone is continuously resorbed by osteoclasts, resulting in bone cavities in which osteoblasts form new bone matrix. This circular process is called remodeling and is a strictly controlled process, which is in balance in a healthy skeletal condition and unbalanced under pathological conditions.

The osteoclast is a bone tissue-specific macrophage polykaryon created by the differentiation of monocyte/macrophage precursor cells in, or in the vicinity of, bone tissue. Osteoclast differentiation is coordinated by bone cells with mesenchymal origin, which include stromal cells, osteoblasts, and matrix-embedded late osteoblasts called osteocytes (1, 2). One of the three known key molecules used by stromal cells/osteoblasts to control osteoclast formation is M-CSF, which binds to c-fms receptors on osteoclast precursor cells and is crucial for the survival and proliferation on these cells. A lack of osteoclasts is observed in osteopetrotic *op*/*op* mutant mice, which lack functional M-CSF (3). The other two cytokines of importance are RANKL (receptor activator of nuclear factor κβ ligand), which binds to RANK (receptor activator of nuclear factor κB) on preosteoclasts, and the decoy receptor osteoprotegerin, which can inhibit osteoclast formation by blocking the interaction between RANKL and RANK (4). Similar to many cytokines and hormones with the capacity to regulate osteoclast formation, the osteotropic hormones parathyroid hormone (PTH)[2] and

* This work was supported by Swedish Research Council 2010-4286 Grant (to P.-A. O.), the Faculty of Medicine of Umeå University, a Young Researcher Award from Umeå University (to P.-A. O.), the Swedish Dental Society, and the County Council of Västerbotten.

[1] To whom correspondence should be addressed: Dept. of Odontology, Sect. for Molecular Periodontology, Umeå University, SE-901 87 Umeå, Sweden. Tel.: 46-90-785-62-94; Fax: 46-90-13-92-89; E-mail: pernilla.lundberg@odont.umu.se.

[2] The abbreviations used are: PTH, parathyroid hormone; BMC, bone marrow culture(s); MEM, minimal essential medium; TRAP, tartrate-resistant acid phosphatase; BMP-2, bone morphogenetic protein 2; PPARγ2, peroxisome proliferator-activated receptor γ2; ALP, alkaline phosphatase; BS, bone surface; ANOVA, one-way analysis of variance; BMM, bone marrow myeloid precursor cell(s).

1α,25(OH)$_2$-vitamin D3 (D3) target osteoblasts and stromal cells causing increased expression and release of RANKL and, therefore, indirectly increase the number of osteoclasts (5). Binding of RANKL to its receptor RANK activates different signaling cascades inducing *nfatc1* (nuclear factor of activated T cells c1), the key transcription factor in osteoclastogenesis. *Nfatc1*, in cooperation with several other transcription factors, induces the transcription of osteoclast-specific genes, including *Trap/Acp5* (tartrate-resistant acid phosphatase), *catK* (cathepsin K), *oscar* (osteoclast-associated receptor), and *ctr* (calcitonin receptor) (5).

Osteoblasts are mononucleated cells derived from pluripotent mesenchymal stem cells, which prior to osteoblast commitment also can differentiate into other mesenchymal cell lineages such as bone marrow stromal cells, fibroblasts, chondrocytes, myoblasts, and adipocytes, depending on the activated signaling transcription pathways. The bone morphogenetic protein 2 (BMP-2) is an example of a potent cytokine, which stimulates osteoblast differentiation and increases bone formation, whereas the peroxisome proliferator-activated receptor γ2 (PPARγ2) is essential in directing the differentiation of adipocyte lineage cells. Activation of the transcription factor Runx2 (Runt-related gene 2) is essential for osteoblast differentiation and bone formation. In addition, the transcription factor osterix, supposed to act downstream of Runx2, and other transcription factors also contribute to the control of osteoblastogenesis. Differentiated osteoblasts express matrix proteins (*e.g.* α-1-collagen) and alkaline phosphatase (ALP), a protein associated with mineralization, which also functions as a biochemical marker for osteoblastic differentiation and bone-forming capacity (6, 7).

CD47, a cell surface glycoprotein of the Ig superfamily and ubiquitously expressed in the body, was originally discovered as an integrin-associated protein important for regulation of at least β1, β3, and β5 integrin members. In addition, CD47 has been suggested to function as a receptor for thrombospondin (8), and as a ligand for signal regulatory protein α (SIRPα) (9). SIRPα is also an Ig superfamily cell surface glycoprotein shown to be highly expressed in myeloid cells, neurons, endothelial cells, and fibroblasts, but not by T cells or B cells. By binding to CD47 on other cells, SIRPα can regulate macrophage-macrophage adhesion, fusion, and formation of giant cells (10, 11).

We have previously shown that osteoclast formation is reduced both *in vivo* and *in vitro* in the absence of CD47 (12). These findings have been confirmed *in vitro* both by Uluçkan *et al.* (13) and Maile *et al.* (14). However, Maile *et al.* did not find any reduction in number of osteoclasts *in vivo* (14). To determine the role of CD47 in bone homeostasis, both *in vitro* and *in vivo*, we here investigated whether CD47 is involved in osteoclast and stromal cell/osteoblast differentiation in murine bone marrow cultures. In addition, we studied osteoblast numbers and bone homeostasis in *CD47*$^{-/-}$ mice.

EXPERIMENTAL PROCEDURES

CD47$^{-/-}$ *Mice and SIRPα Mutant Mice*—Generation of *CD47*$^{-/-}$ has been described previously (15). Male *CD47*$^{-/-}$ Balb/c mice, backcrossed to Balb/c (The Jackson Laboratory, Bar Harbor, ME) for 16 or more generations, and their wild-type homozygous littermates were from our own breeding colony. C57BL/6 SIRPα mutant mice, lacking most of the SIRPα cytoplasmic domain were described previously (16, 17). Male SIRPα mutant mice or their wild-type littermates, backcrossed for >10 generations, were from our own breeding colony. Animals were kept in accordance with local guidelines and maintained in a specific pathogen-free barrier facility. The Local Animal Ethics Committee approved all animal procedures.

Bone Marrow Cell Culture (BMC)—Bone marrow cells were isolated from femurs and tibiae of Balb/c mice, 5–9 weeks of age (*CD47*$^{+/+}$ and *CD47*$^{-/-}$) and seeded on 48- or 12-well plates (Nunc, Roskilde, Denmark) in α-MEM with 10% FCS (Invitrogen), L-glutamine, and antibiotics (Sigma Aldrich), with cell concentration of 10^6 cells/cm^2. The number of mice used for each experiment differed between 1–4 depending on the size of the experiment. If more than one mouse was used, the bone marrow cells were pooled. After 24 h (day 0) of incubation (37 °C, 5% CO_2), the medium was replaced and either PTH 10^{-8} M (Bachem, Bubendorf, Switzerland), D3 10^{-8} M (Roche Diagnostics, Mannheim, Germany), or BMP-2 125 ng/ml (R&D Systems, Abdingdon, UK) were added to the cultures. At day 3, medium and test substances were changed. On days 6–7, the cultures were harvested, and the cells were either lysated for further RNA isolation or fixed with acetone in citrate buffer and subsequently stained for TRAP as described below.

Osteoclast Formation and Resorption on Bone Slices—Bone marrow cells were isolated as described above. Thereafter, the cells were seeded on bone slices in 96-well tissue culturing plates (Nunc, Roskilde, Denmark) in α-MEM with 10% FCS (Invitrogen), L-glutamine and antibiotics (Sigma Aldrich), with cell concentration of 10^6 cells/cm^2. The cells were incubated for 24 h (37 °C, 5% CO_2), and thereafter, the medium was changed and D3 10^{-8} M (Roche Diagnostics) was added. Medium was changed every third day, and after 10 days of culture, the experiments were harvested and stained for TRAP positivity, osteoclasts were counted in a light microscope, and resorption pits were visualized by an external light source. Moreover, the release of collagen type I fragments into the culture medium during resorption was analyzed by CrossLaps according to the manufacturer's instructions.

Osteoblast Differentiation—Bone marrow cells were isolated and plated as in above described BMC and plated in 24-well tissue culturing plates (Nunc, Roskilde, Denmark). The cells were cultured in α-MEM with 10% FCS (Invitrogen), L-glutamine, and antibiotics (Sigma Aldrich). The medium was changed every third day. At day 6, the culture medium was replaced with osteoblastic differentiation medium (α-MEM with 10% FCS, L-glutamine, antibiotics, 10 mM β-glycerol phosphate, and 50 μg/ml ascorbic acid). At days 7, 14, and 21, the cells were fixed with acetone in citrate buffer and stained for ALP or von Kossa as described below.

Bone Marrow Stromal Cell Culture—Bone marrow cells were isolated and treated as in BMC except that they were plated in 60 cm^2 culture dishes (Nunc). The cells were cultured in α-MEM with 10% FCS (Invitrogen), L-glutamine, antibiotics (Sigma Aldrich). The medium was changed after 3 days. After 7 days, the adhering cells were detached, counted, and plated at a concentration of 2×10^4 cells/cm^2 in 24-well and 12-well tissue

culturing plates (Nunc). The cells were either lysed for further RNA isolation or stained for ALP or von Kossa at the stated culture time.

Co-culture—Cells used for co-culture experiments were harvested from mice, 5–9 weeks of age, either Balb/c (*CD47*$^{+/+}$ and *CD47*$^{-/-}$) or C57BL/6 wild-type or SIRPα mutants. Bone marrow cells were isolated and treated as in BMC except that they were plated in 60 cm^2 culture dishes (Nunc). The cells were cultured in α-MEM with 10% FCS (Invitrogen), L-glutamine, and antibiotics (Sigma Aldrich). Medium was changed every third day, and after 14 days, the adherent cells were trypsinated, counted, and seeded at 10^5 cells/cm^2, in 96-well tissue culturing plates (Nunc) and thereafter incubated for 24 h (37 °C, 5% CO_2). Meanwhile non-adherent bone marrow myeloid precursor cells were isolated by flushing out bone marrow from femurs and tibiae. Following lysis of erythrocytes, the remaining cells were plated in 60 cm^2 tissue culture-treated culture dishes (Nunc) and kept at 37 °C for 2 h. Thereafter, the non-adherent cells were collected, counted, and seeded onto the stromal cells at 6×10^4 cells/cm^2. The co-cultures were stimulated with D3 10^{-8} M (Roche Diagnostics, Mannheim, Germany). After 5–7 days, the cultures were harvested, fixed, and stained for TRAP as described below.

TRAP staining was performed by use of the leukocyte acid phosphatase kit (Sigma-Aldrich) according to the manufacturer's instructions. TRAP$^+$ cells with three or more nuclei were considered osteoclasts, and the number of multinucleated osteoclasts was counted in a light microscope.

ALP and von Kossa Staining—Osteoblast differentiation was visualized with ALP staining by using Naphtol AS-MX phosphate, disodium salt, and Fast Blue BB (Sigma Aldrich) according to histochemical standard procedure. Mineralization of extracellular matrix was visualized by von Kossa staining with 2% silver nitrate (Fisher Scientific UK) under UV light for 30 min. The result of ALP and von Kossa staining was photographed.

RNA Isolation and First-stranded cDNA Synthesis—Total RNA from adherent bone marrow cell cultures was isolated by using the RNAqueous®-4PCR kit (Ambion, Austin, TX) according to the manufacturer's instructions. By using the high capacity cDNA reverse transcription kit (Foster City, CA), mRNA was reverse-transcribed to cDNA.

Quantitative Real-time PCR—To detect and analyze gene expression, Taq-man (API PRISM 7900HT Sequence Detection System) was used. The expression of *Trap/Acp5*, *ctr*, *catK*, *nfatc1*, *oscar*, *dc-stamp*, *c-fms*, *rank*, *rankl*, *m-csf*, *SIRPα*, *runx-2*, osterix, α-1-collagen, *Alp*/*Akp1*, *PPARγ* and osteoprotegerin were analyzed in BMC. To control variability in amplification due to differences in starting mRNA-concentrations, β-actin was used as housekeeping gene.

ELISA—The amount of synthesized protein of RANKL and M-CSF in culture medium was assessed by measuring the levels of the proteins in BMC using commercially available ELISA kits. RANKL was measured according to manufacturer's instructions (R&D Systems) and M-CSF according to the manufacturer's instructions (AB Frontier, Seoul, Korea).

TRAP Activity Assay—BMC were washed three times in PBS and lysed in Triton X-100 (0.2% in H_2O). By using *p*-nitrophenol phosphate (1.7 mg/ml) as substrate at pH 4.9 in the presence of tartrate (0.17 M), the TRAP activity was determined. The activity of the enzyme was assessed as the A_{405}. The enzyme assay was performed under conditions where the reaction was proportional to amount of enzyme and reaction time.

ALP Activity Assay—Alkaline phosphatase was measured in BMC stimulated with BMP-2 by using a commercially available kit (Sigma Aldrich).

Flow Cytometric Analysis—Bone marrow stromal cells were washed and resuspended in cold PBS. Fifty μl of the cells (1×10^5 cells) were seeded in a 96-well V-bottomed plate and centrifuged at 1500 rpm for 3 min at 4 °C. Thereafter, the cells were resuspended in 30 μl staining buffer (PBS + 2% FCS) containing saturating concentrations of Alexa Fluor 488-conjugated anti-SIRPα mAb P84, or Alexa Fluor 488-conjugated rat IgG isotype control mAb, for 30 min on ice. Cells were then washed once with 200 μl of cold PBS, resuspended in cold PBS/2% FCS/0.05% NaN_3, and analyzed by flow cytometry (FACS Calibur, Becton Dickinson) and CellQuest software (Beckton Dickinson).

Immunoprecipitation and Western Blot—Bone marrow stromal cells, cultured for 14 days, were lysed with ice-cold lysis containing 20 mM Hepes (pH 7.4), 150 mM NaCl, 1 mM EGTA, 1% Nonidet P-40 (Pierce), 1% of proteinase inhibitor mixture (Sigma), 0.5 μM pervanadate, and 1 mM phenylmethylsulfonyl fluoride. Immunoprecipitation with the anti-SIRPα mAb P84 was done essentially as described previously. In brief, cell lysates were incubated with mAb P84-coated protein G-Sepharose overnight at 4 °C. Washed immunoprecipitates were boiled for 5 min in reduced SDS-PAGE sample buffer with β-mercaptoethanol and separated on 10% SDS-PAGE, followed by transfer to nitrocellulose under standard conditions. Nonspecific binding was blocked by 3% nonfat dry milk in TBST (50 mM Tris, 150 mM NaCl, 0.1% Tween 20 (pH 7.6)) followed by immunoblotting with anti-SIRPα mAb P84 or anti-phosphotyrosine mAb 4G10 (Millipore). Primary antibodies were detected with peroxidase-conjugated goat anti-rat or anti-mouse mouse IgG, and detection of signals was by chemiluminescence (ECL, Amersham Biosciences).

Phenotypic Studies—Histomorphometry and peripheral quantitative computed tomography were used to analyze the bone phenotype of male BalbC *CD47*$^{-/-}$ mice at the age of 18 and 28 weeks and compared with normal mice at the same age.

Histomorphometry—*CD47*$^{+/+}$ or *CD47*$^{-/-}$ mice were injected with the fluorescent compound calcein (15 mg/kg; Sigma) 10 days and 3 days prior to collection, respectively. At 18 and 28 weeks of age *CD47*$^{+/+}$ and *CD47*$^{-/-}$ were euthanized by cervical dislocation. Both femurs were excised and bisected transversely at the midpoint of the shaft. The distal halves of the right femora were fixed and embedded, undecalcified in methyl-methacrylate resin (Medim-Medizinische Diagnostik, Giessen, Germany), and 5-μm sagittal sections were prepared for analysis using Q Win software (Leica Microsystems Pty., Ltd., Sydney, Australia). Sagittal sections were stained for mineralized tissue, and trabecular bone volume, trabecular thickness, and trabecular number were calculated in a sample region extending 4.5 mm proximal to the distal growth plate and encompassing all trabecular bone within the cortical boundaries. Osteoblast

parameters (osteoblast surface, osteoblast number, and osteoid surface) were estimated using sections stained with von Kossa stain and toluidine blue. Only osteoblasts identified adjacent to osteoid surfaces were included in the analysis. Bone formation (mineralizing surface, MS) was estimated using the bone surface (BS) coverage of single- and double-labeled (sLS and dLS) fluorescent bands using the equation MS = ((0.5 × sLS) + dLS) × 100/BS, expressed as a percentage of bone surface. Mineral apposition rate (MAR) was estimated by the distance between the calcein labels divided by the time interval between injections of labels (MAR = interlabel distance divided by 7, expressed in μm/day). Bone formation rate (BFR) was calculated after fluorescence microscopy (Leica Microsystems, Heerbrugg, Switzerland) as BFR = MS/bone surface × MAR, expressed in $\mu m^2/\mu m^3$/day. For measurements of osteoclast surface and osteoclast number, sections were stained for TRAP positivity.

Peripheral quantitative computed tomography was used to analyze cortical bone of the tibia, using a Stratec XCT Research SA scanner (Stratec Medizintechnik, Pforzheim, Germany). Scans were conducted using a voxel size of 70 μm, scan speed of 5 mm/s and slice width of 1 mm on excised tibia, as described previously (18). Bones were scanned in a single slice 4 mm distal from the proximal margin of the tibia.

Micro-computed Tomography—A Skyscan 1174 scanner and associated analysis software (Skyscan, Aartselaar, Belgium) were used to visualize the three-dimensional bone structure of the distal femoral metaphysis. Following fixation, representative bones were scanned in 70% ethanol. A 0.5-mm aluminum filter was applied to the 50 kV x-ray source, with an exposure time of 3600 ms and sharpening at 40%. Distal femora were scanned at a 6.2 μm pixel resolution acquired over an angular range of 180°, with a rotation step of 0.4°. Following reconstruction, 67-μm-thick images were created from a point 400 μm from the most proximal aspect of the growth plate.

Statistical Analyses—The statistical analyses were performed using one-way analysis of variance (ANOVA) with Levene's homogenicity test, and post hoc Bonferroni's test or, where appropriate, Dunnett's *t* test. Students *t* test were used in the histomorphometric analyses (SPSS, version 18). All experiments were performed at least twice with comparable results, and all data are represented as the means ± S.E. Significance levels were set to $p < 0.05$ (*), 0.01 (**), or 0.001 (***).

RESULTS

CD47 Is Required for Functional Osteoclast Differentiation in Vitro—We have previously shown that mice lacking CD47 have reduced numbers of osteoclasts on trabecular bone surfaces *in vivo* (12). To further elucidate the role of CD47 in osteoclastogenesis within the bone marrow, we studied $CD47^{-/-}$ or $CD47^{+/+}$ crude BMC, containing both mesenchymal/stromal cells and hematopoietic cells, to mimic the *in vivo* situation. Addition of PTH (10^{-8} M) or D3 (10^{-8} M) stimulated formation of multinucleated osteoclasts in $CD47^{+/+}$ BMC ($n = 96 \pm 15.8$ and 142 ± 14.1, respectively) (Fig. 1, *A* and *B*). In marked contrast, only a few multinucleated osteoclasts were detected in PTH or D3-stimulated $CD47^{-/-}$ cultures ($n = 4 \pm 1.1$ and $n = 8 \pm 3.2$, respectively) (Fig. 1, *A* and *B*). When $CD47^{-/-}$ BMC were cultured on bone slices, we found both fewer osteoclasts (Fig. 1*C*) and dramatically fewer resorption pits reflected as an 82% reduced release of collagen type I fragments into the culture medium, as compared with that in $CD47^{+/+}$ cultures (Fig. 1*D*). *Trap*/*Acp5* mRNA and TRAP protein expressions were substantially increased in $CD47^{+/+}$ BMC in response to PTH (10^{-8} M) or D3 (10^{-8} M), whereas no (D3), or only a slight (PTH) ($p < 0.001$), increase in TRAP protein expression was seen in $CD47^{-/-}$ cultures (Fig. 2, *A* and *B*). Quantitative real-time PCR analyses of $CD47^{+/+}$ BMC revealed that D3 substantially stimulated the mRNA expression of *ctr* and *catK*, whereas D3 did not increase *ctr* expression and only marginally increased *catK* expression ($p < 0.05$) in $CD47^{-/-}$ cultures (Fig. 2, *C* and *D*). The mRNA expression of *nfatc1*, the master transcription factor regulating osteoclastogenesis, and the osteoclast-associated receptor *oscar*, were both increased in D3-stimulated $CD47^{+/+}$ cultures but not in $CD47^{-/-}$ cultures (Fig. 3). D3 did not significantly regulate the mRNA expression of the receptors *c-fms* or *SIRPα*, and no significant difference was seen comparing the two genotypes (Fig. 3). However, we found that the mRNA expression of *rank* was up-regulated in $CD47^{+/+}$ BMC stimulated with D3 ($p < 0.001$), whereas no such response to D3 was seen in $CD47^{-/-}$ BMC (Fig. 3). Additionally, the mRNA expression of dendritic cell-specific transmembrane protein (*dc-stamp*), a protein of importance for osteoclast fusion was substantially increased in response to D3 in the $CD47^{+/+}$ cultures ($p < 0.05$; Fig. 3), whereas only a minor increase was seen in $CD47^{-/-}$ cultures ($p < 0.05$; Fig. 3).

Because production of M-CSF in BMC-cultures is pivotal for osteoclastogenesis due to its capacity to increase survival of osteoclast progenitor cells (3), we next investigated whether this function was impaired in $CD47^{-/-}$ BMC. These experiments revealed that *m-csf* gene expression was significantly reduced in unstimulated $CD47^{-/-}$ BMC cultures, as compared with that in unstimulated $CD47^{+/+}$ BMC ($p < 0.05$; Fig. 4*A*). By comparing M-CSF protein levels in culture medium from $CD47^{+/+}$ or $CD47^{-/-}$ cultures, we confirmed a significantly lower concentration of M-CSF, both in control and D3-stimulated $CD47^{-/-}$ cultures (Fig. 4*B*). The effect of D3 on M-CSF expression in BMC is to our knowledge unknown, but in our experiments, D3 seems to decrease the M-CSF expression in the normal mice. Analyses of RANKL expression in D3-stimulated $CD47^{+/+}$ BMC revealed a significant increase in *rankl* mRNA, as well as RANKL protein in culture medium, whereas no such response to D3 was detected in $CD47^{-/-}$ cultures with the exception of a very slight but significant increase ($p < 0.01$) in the protein levels of RANKL in $CD47^{-/-}$ culture medium (Fig. 4, *C* and *D*). When stimulating BMC cultures with D3, the osteoprotegerin protein expression decreased in both $CD47^{-/-}$ and $CD47^{+/+}$ cultures (data not shown), and thus, the RANKL/osteoprotegerin-ratio increased in both genotypes.

CD47 Is Required for Osteoblastogenesis and Bone Formation in Vitro—The strongly reduced production of M-CSF and RANKL in $CD47^{-/-}$ cultures indicated a stromal cell differentiation defect when CD47 was absent. Therefore, we next analyzed osteoblastic differentiation in BMC and found that the major transcription factors for osteoblast differentiation, *runx2* and osterix, were increased over time in $CD47^{+/+}$ cultures

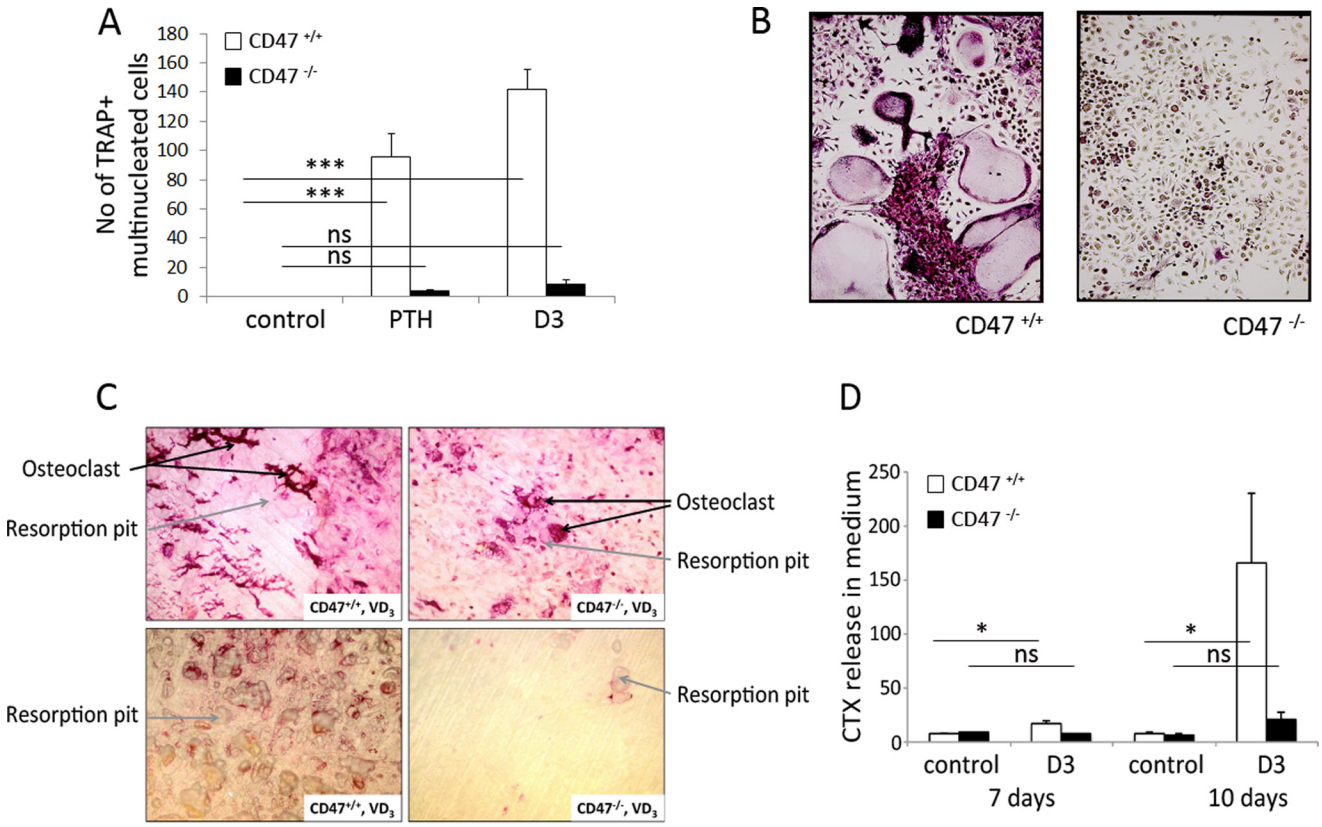

FIGURE 1. **Strongly reduced osteoclast differentiation, osteoclast formation, and bone resorption in *CD47*$^{-/-}$ BMC.** *A*, significantly fewer osteoclasts were formed in *CD47*$^{-/-}$ BMC stimulated with PTH (10^{-8} M) or D3 (10^{-8} M), as compared with that in *CD47*$^{+/+}$ BMC. Data in *A* are the means ±S.E. of four to six samples/group in one of five representative experiments. *B*, representative photomicrographs showing the difference in TRAP^{+} multinucleated osteoclasts between *CD47*$^{-/-}$ and *CD47*$^{+/+}$ BMC after 6 days of culture. Cells that contained three or more nuclei and stained *red/purple* were counted as TRAP^{+} multinucleated osteoclasts. BMC performed on bone slices, stimulated with D3, showed both fewer osteoclasts and resorption pits in *CD47*$^{-/-}$ cultures compared with *CD47*$^{+/+}$, which is illustrated by representative photomicrographs (*A*) and subsequently significantly lower release of collagen type I fragments (*CTX*) in culture medium in *CD47*$^{-/-}$ cultures compared with *CD47*$^{+/+}$ cultures (*B*). Data in *B* are means ± S.E. of four to six samples/group in one of two representative experiments. *ns*, not significant. *, $p < 0.05$ and ***, $p < 0.001$, using Student's *t* test or ANOVA with Levene's homogenicity test and post hoc Bonferroni's test or, where appropriate, Dunnett's *t* test.

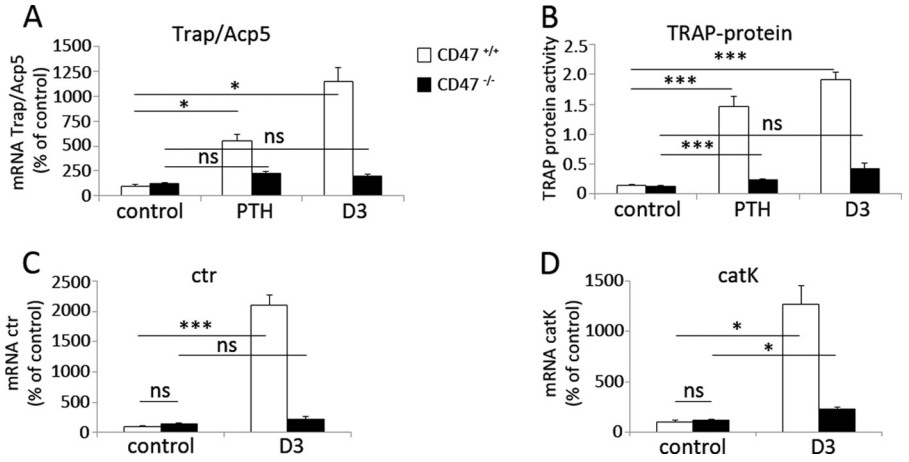

FIGURE 2. **Impaired expression of osteoclast-specific genes in *CD47*$^{-/-}$ BMC.** *A* and *B*, the mRNA expressions of Trap/Acp5, as well as the TRAP protein activity, were significantly increased in *CD47*$^{+/+}$ BMC when stimulated with either PTH or D3, whereas expressions of *Trap/Acp5* mRNA or TRAP protein were markedly blunted in PTH or D3-stimulated *CD47*$^{-/-}$ BMC. Data in *A* and *B* are the means ± S.E. of four to six samples/group in one of three representative experiments. *C*, the expression of *ctr* was significantly increased in *CD47*$^{+/+}$ BMC, but not in *CD47*$^{-/-}$ BMC following D3 stimulation. *D*, enhanced *catK* expression in D3-stimulated *CD47*$^{+/+}$ BMC, as compared with that in *CD47*$^{-/-}$ BMC. Data in *C* and *D* are means ± S.E. of four to six samples/group in one of two representative experiments. The mRNA expression data shown in *A*, *C*, and *D* are quantitative values normalized to the housekeeping gene β-actin. The *CD47*$^{+/+}$ control was set to 100%. *, $p < 0.05$ and ***, $p < 0.001$, using ANOVA with Levene's homogenicity test and post hoc Bonferroni's test or, where appropriate, Dunnett's *t* test. *ns*, not significant.

(Fig. 5*A*). However, in *CD47*$^{-/-}$ cultures, we observed no increase in osterix mRNA expression and only a modest increase in *runx2* mRNA expression (Fig. 5*A*). Moreover, although the expression of *Alp*/*Akp1* and α-1-collagen substantially increased over time in *CD47*$^{+/+}$ BMC, no significant increase of *Alp*/*Akp1* and only a small increase in α-1-collagen were seen in *CD47*$^{-/-}$ cultures (Fig. 5*B*). Thus, the mRNA expression of *Alp*/*Akp1* and α-1-collagen were significantly

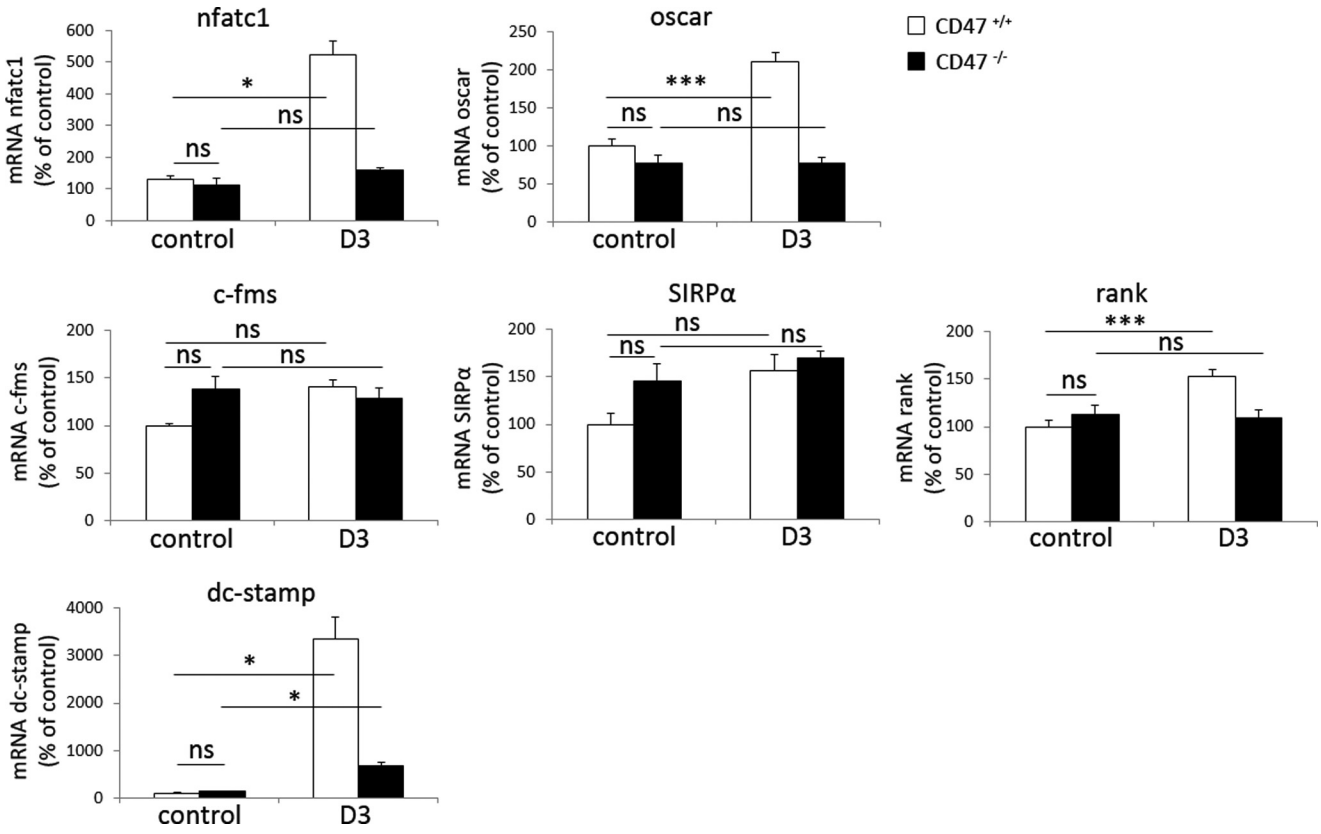

FIGURE 3. **Impaired expression of osteoclast differentiation-associated genes in *CD47*$^{-/-}$ BMC.** The expression of *nfatc1*, *oscar*, rank, and *dc-stamp* were all significantly increased when stimulating *CD47*$^{+/+}$ BMC with D3 (10^{-8} M). With the exception of *dc-stamp*, which was weakly but statistically significantly increased, neither of these genes were up-regulated in D3-stimulated *CD47*$^{-/-}$ BMC. The mRNA expression of *c-fms* or *SIRPα* were not significantly up-regulated when stimulating BMC from *CD47*$^{+/+}$ or *CD47*$^{-/-}$ with D3 (10^{-8} M). The *CD47*$^{+/+}$ control was set to 100%, and data shown are quantitative values normalized to the housekeeping gene *β*-actin. All genes were analyzed in two or more different experiments, and the data shown are the means ± S.E. of four to six samples/group in one representative experiment. *ns*, not significant. *, $p < 0.05$ and ***, $p < 0.001$, using ANOVA with Levene's homogenicity test and post hoc Bonferroni's test or, where appropriate, Dunnett's *t* test.

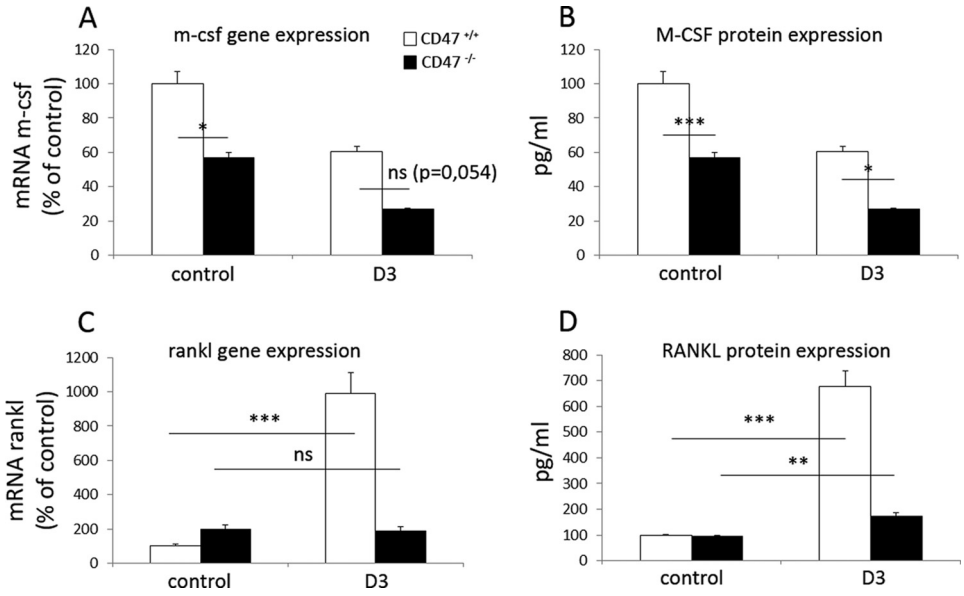

FIGURE 4. **Reduced expression of M-CSF and RANKL in D3-stimulated *CD47*$^{-/-}$ BMC.** The mRNA expression of *m-csf* (*A*), as well as M-CSF protein in culture medium (*B*), were lower both in control and D3-stimulated *CD47*$^{-/-}$ BMC, as compared with that in *CD47*$^{+/+}$ BMC. In D3-stimulated *CD47*$^{+/+}$ BMC, both *rankl* mRNA expression (*C*) and RANKL protein in culture medium (*D*) were strongly increased, as compared with that in *CD47*$^{-/-}$ BMC. The unstimulated *CD47*$^{+/+}$ control was set to 100%, and data of mRNA analyses are quantitative values normalized to the housekeeping gene *β*-actin. All genes were analyzed in two or more different experiments, and the data shown are the means ± S.E. of four to six samples/group in one representative experiment. *ns*, not significant. *, $p < 0.05$; **, $p < 0.01$; and ***, $p < 0.001$, using ANOVA with Levene's homogenicity test and post hoc Bonferroni's test or, where appropriate, Dunnett's *t* test.

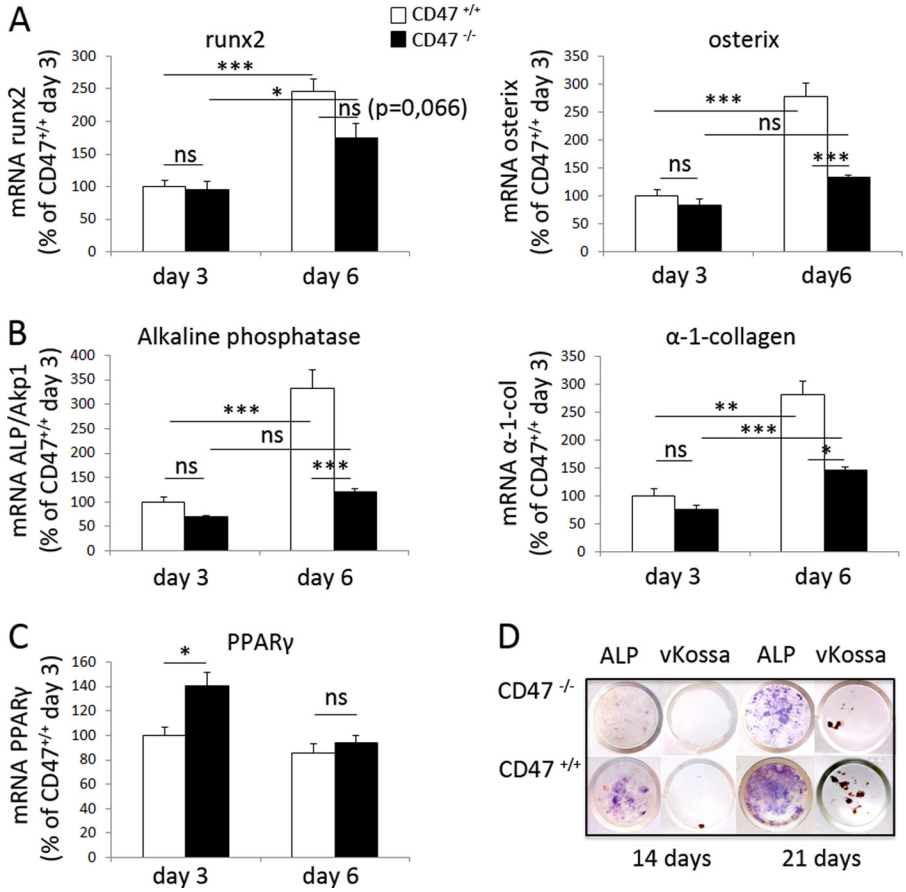

FIGURE 5. **Impaired expression of osteoblast-specific genes and osteoblast differentiation in *CD47*$^{-/-}$ BMC.** *A* and *B*, the mRNA expression of *runx2*, osterix, *Alp/Akp1*, and α-1-collagen were significantly increased from day 3 to 6 during culture of *CD47*$^{+/+}$ BMC. With the exception of *runx2*, these responses were significantly lower in *CD47*$^{-/-}$ BMC, as compared with *CD47*$^{+/+}$ BMC. *C*, the expression of the adipocytic gene *PPARγ* was higher in *CD47*$^{-/-}$ cultures, as compared with that in *CD47*$^{+/+}$ cultures on day 3 but not on day 6. Data shown are quantitative values normalized to the housekeeping gene β-actin, where the *CD47*$^{+/+}$ control day 3 was set to 100%. All genes were analyzed in two or more different experiments, and the data shown are the means ± S.E. of four to six samples/group in one representative experiment. *ns*, not significant. *, $p < 0.05$; **, $p < 0.01$; and ***, $p < 0.001$, using ANOVA with Levene's homogenicity test and post hoc Bonferroni's test or, where appropriate, Dunnett's *t* test. *D*, representative photographs of ALP staining (*purple*) and von Kossa staining (*brown* mineral deposits) in BMC from both *CD47*$^{+/+}$ and *CD47*$^{-/-}$ mice after 14 and 21 days of culture in osteogenic medium supplemented with β-glycerophosphate and ascorbic acid.

lower in *CD47*$^{-/-}$ BMC when compared with *CD47*$^{+/+}$ BMC. Interestingly, at day 3 of culture, we found a slight up-regulation of the adipocyte-specific gene PPARγ expression in *CD47*$^{-/-}$ cultures, as compared with *CD47*$^{+/+}$ cultures, whereas no difference in *PPARγ* expression was seen at day six of culture (Fig. 5*C*).

We further analyzed the stromal cell differentiation capacity in *CD47*$^{-/-}$ BMC by culturing the cells in osteogenic medium supplemented with β-glycerophosphate and ascorbic acid. Under these conditions, *CD47*$^{+/+}$ BMCs were positive for the osteoblastic marker ALP at day 14 of culture, when small spots of mineral deposits were also detected (Fig. 5*D*). In marked contrast, less ALP-staining and no mineral deposits were seen at day 14 in *CD47*$^{-/-}$ BMC cultures (Fig. 5*D*). By 21 days of culture, the ALP expression and mineral deposits increased in both *CD47*$^{+/+}$ and *CD47*$^{-/-}$ cultures, but the expression of ALP and formation of mineral were still much lower in *CD47*$^{-/-}$ cultures (Fig. 5*D*).

Because BMP-2 is a known stimulator of osteoblastic differentiation (19), we next investigated the effects of exogenous BMP-2 on BMC differentiation toward the osteoblastic lineage. As shown in Fig. 5*D*, culture of *CD47*$^{+/+}$ BMC for 6 days in osteogenic medium alone induced ALP protein expression, as compared with the virtual lack of ALP expression in *CD47*$^{-/-}$ cultures. Addition of BMP-2 induced a robust increase in ALP protein expression in *CD47*$^{+/+}$ BMC, whereas the ALP was maintained at extremely low levels in BMP-2-stimulated *CD47*$^{-/-}$ cultures (Fig. 6, *A* and *B*). Furthermore, there was a marked difference in cellular morphology between the two genotypes. In both unstimulated and BMP-2-stimulated *CD47*$^{+/+}$ BMC, the vast majority of the cells showed spreading on the plastic surface. However, cell spreading appeared to be strongly reduced in unstimulated as well as BMP-2-stimulated *CD47*$^{-/-}$ cultures (Fig. 6*B*).

Tyrosine phosphorylation of SIRPα, for which CD47 is a ligand, is important in mediating adhesion-dependent cellular functions (16). In endothelial cells, adhesion-dependent SIRPα tyrosine phosphorylation requires CD47 (20). Therefore, we next investigated whether impaired signaling through SIRPα could be involved in mediating the reduced osteoblast differentiation in *CD47*$^{-/-}$ cultures. Flow cytometric analysis of bone marrow stromal cells showed that SIRPα was expressed at equal levels by both *CD47*$^{+/+}$ and *CD47*$^{-/-}$ stromal cells (Fig. 6*C*). When SIRPα was immunoprecipitated from stromal cell cultures of *CD47*$^{+/+}$ or *CD47*$^{-/-}$ mice, a strong tyrosine phos-

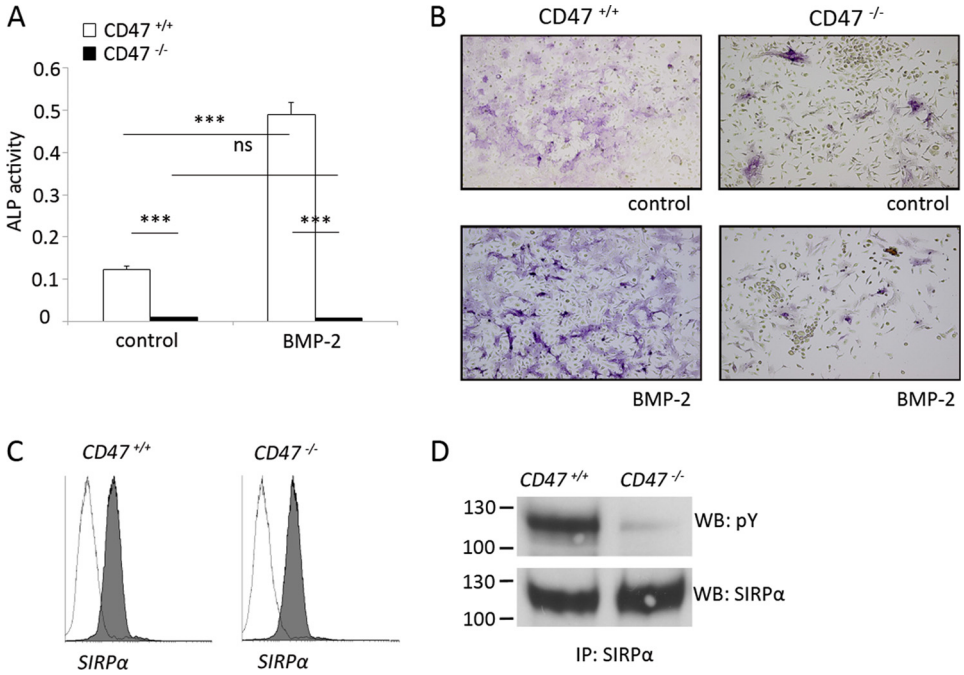

FIGURE 6. **Blunted osteoblast differentiation in *CD47*$^{-/-}$ stromal cells is associated with the lack of SIRPα tyrosine phosphorylation.** *A*, ALP protein expression was evident following 6 days of *CD47*$^{+/+}$ BMC culture in osteogenic medium alone (control) and significantly increased in cultures stimulated for 6 days with BMP-2 (125 ng/ml). *CD47*$^{-/-}$ BMC expressed remarkably little ALP protein when cultured in osteogenic medium and were unresponsive to BMP-2. *B*, representative photomicrographs showing purple ALP^{+} cells in *CD47*$^{+/+}$ or *CD47*$^{-/-}$ BMC cultured in osteogenic medium alone (control), or in BMC stimulated with BMP-2 (125 ng/ml) stimulated at 6 days of culture. ALP^{+} cells are stained *blue*. Data are shown as the means ± S.E. of four to six samples/group in one of two representative experiments. *ns*, not significant. ***, $p < 0.001$, using ANOVA with Levene's homogenicity test and post hoc Bonferroni's test or, where appropriate, Dunnett's *t* test. *C*, flow cytometric analysis of cell surface SIRPα expression in *CD47*$^{+/+}$ or *CD47*$^{-/-}$ bone marrow stromal cells cultured for 14 days. Cells were labeled with anti-SIRPα mAb P84 (*gray* histogram) or isotype rat IgG1 mAb (*open* histogram), where both antibodies were conjugated to Alexa Fluor 488. *D*, adherent bone marrow stromal cells derived from *CD47*$^{+/+}$ or *CD47*$^{-/-}$ mice and cultured for 14 days were lysed, and SIRPα was immunoprecipitated from equal amounts of protein. The tyrosine phosphorylation (*pY*) of SIRPα immunoprecipitated from stromal cells of each genotype was determined by Western blot (*WB*), using anti-phosphotyrosine mAb 4G10. Equal loading of SIRPα immunoprecipitates was confirmed by blotting for SIRPα using mAb P84. The data are representative of two separate experiments with virtually identical results.

phorylation of SIRPα was detected in *CD47*$^{+/+}$ cells, whereas the SIRPα phosphorylation was virtually blunted in *CD47*$^{-/-}$ cells (Fig. 6*D*). Thus, lack of SIRPα tyrosine phosphorylation in *CD47*$^{-/-}$ stromal cells could explain the reduced osteoblastic differentiation in *CD47*$^{-/-}$ BMC. To further challenge this hypothesis, we investigated differentiation of bone marrow stromal cells from SIRPα-mutant mice. These mice express normal levels of CD47 as well as the SIRPα extracellular domain, but the cytoplasmic SIRPα domain is deleted and cannot be phosphorylated upon ligation of the receptor (17). Interestingly, ALP protein expression was strongly reduced in SIRPα mutant BMC cultured for 12 days, as compared with that in SIRPα wild-type cultures (data not shown). Thus, osteogenic differentiation of bone marrow stromal cells requires CD47-dependent SIRPα signaling.

Based on these findings, we next hypothesized that the absence of stromal cell CD47, and subsequent lack of SIRPα signaling, could explain the impaired osteoclast formation in D3-stimulated *CD47*$^{-/-}$ BMC. To address this hypothesis, we conducted D3-stimulated co-culture experiments combining bone marrow stromal cells and bone marrow myeloid precursor cells of either genotype (wild-type, *CD47*$^{-/-}$, or SIRPα mutant). These experiments revealed that wild-type and *CD47*$^{-/-}$ myeloid precursor cells generated equal numbers of multinucleated osteoclast on CD47 wild-type bone marrow stromal cells, whereas myeloid precursors of both genotypes generated low numbers of multinucleated osteoclast on *CD47*$^{-/-}$ stromal cells (Fig. 7*A*). Similarly, SIRPα wild-type and SIRPα mutant myeloid precursors gave rise to an equal number of multinucleated cells on SIRPα wild-type bone marrow stromal cells, whereas SIRPα mutant stromal cells showed a strongly reduced ability to promote multinucleated osteoclast formation in both wild-type and SIRPα mutant myeloid precursors (Fig. 7*B*).

Reduced Osteoclast and Osteoblast Numbers and Impaired Skeletal Parameters, in CD47$^{-/-}$ *Mice*—To investigate the biological impact of our *in vitro* observations, we next analyzed osteoclast and osteoblast densities in femoral bones of 18- or 28-week-old male *CD47*$^{+/+}$ or *CD47*$^{-/-}$ mice. We have previously reported a 37% reduction in TRAP^{+} osteoclast surface and a 29% reduction in osteoclast number in the distal femoral metaphysis of 18-week-old *CD47*$^{-/-}$ mice, as compared with that in age-matched *CD47*$^{+/+}$ mice (12). Herein, we further analyzed the osteoclast density in 28-week-old mice and found that *CD47*$^{-/-}$ mice had a 38% ($p < 0.01$) reduction in osteoclast numbers and a 46% ($p < 0.01$) reduction in osteoclast surface, as compared with *CD47*$^{+/+}$ mice (Fig. 8, *A* and *B*). Importantly, osteoblast numbers were also reduced in *CD47*$^{-/-}$ mice, with a 55 and 47% reduction, respectively, in 18- and 28-week-old *CD47*$^{-/-}$ mice, as compared with age-matched *CD47*$^{+/+}$ mice ($p < 0.001$ and $p < 0.01$, respectively; Fig. 8, *C* and *D*).

To further investigate the effects of reduced osteoclastogenesis and osteoblastogenesis in *CD47*$^{-/-}$ mice, trabecular

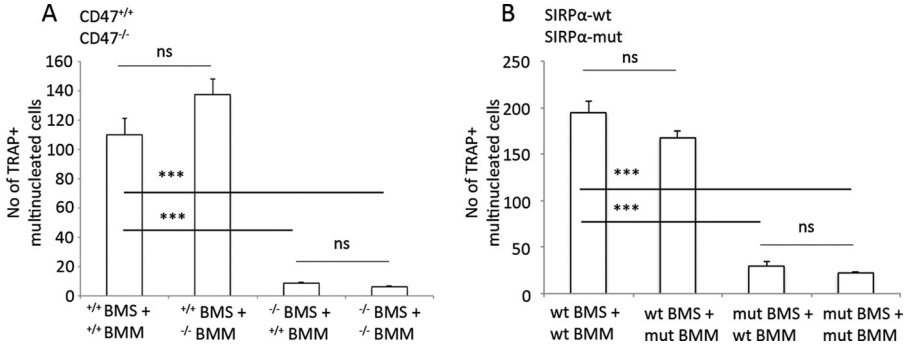

FIGURE 7. **D3-stimulated bone marrow stromal cells lacking CD47, or expressing mutated non-signaling SIRPα, are unable to support osteoclastogenesis.** *A*, *CD47*$^{+/+}$ D3-stimulated (10^{-8} M) BMS induced similar levels of osteoclast formation in both *CD47*$^{+/+}$ and *CD47*$^{-/-}$ non-adherent BMM. In contrast, D3-stimulated *CD47*$^{-/-}$ BMS showed strongly reduced capacity to induce osteoclast formation in non-adherent bone marrow myeloid precursor cells of either genotype. *B*, wild-type D3-stimulated BMS induced osteoclast formation in non-adherent bone marrow myeloid precursor cells from both wild-type and non-signaling SIRPα mutant mice. However, osteoclast formation in non-adherent bone marrow myeloid precursor cells of either genotype was strongly reduced when co-cultured with D3-stimulated BMS expressing the non-signaling SIRPα protein. Data are shown as the means ± S.E. of four to six samples/group in one of two representative experiments. *ns*, not significant. ***, $p < 0.001$, using ANOVA with Levene's homogenicity test and post hoc Bonferroni's test or, where appropriate, Dunnett's *t* test. *mut*, mutant.

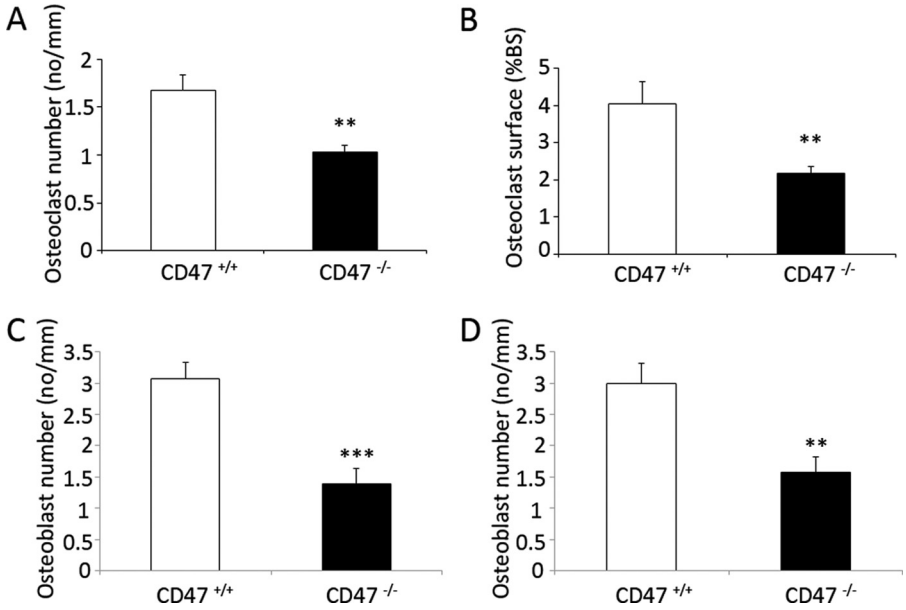

FIGURE 8. **Reduced osteoclast and osteoblast numbers in bones of *CD47*$^{-/-}$ mice.** At 28 weeks of age, the number of osteoclasts covering trabecular bone surface (*A*) and the total osteoclast surface that covers the trabecular bone (*B*) were both significantly reduced in *CD47*$^{-/-}$ mice, as compared with that in *CD47*$^{+/+}$ mice. At both 18 (*C*) and 28 (*D*) weeks of age, the number of osteoblasts covering the bone surface was significantly lower in *CD47*$^{-/-}$ mice, as compared with that in *CD47*$^{+/+}$ mice. Data are means ± S.E. of 7–10 mice in each age group. **, $p < 0.01$ and ***, $p < 0.001$, as compared with that in *CD47*$^{+/+}$ mice, using Student's *t* test for unpaired analyses.

microarchitecture was evaluated both in adult and aged mice bone. Histomorphometric analysis of the distal femurs revealed that the trabecular bone volume was significantly reduced by 15% in 18-week-old *CD47*$^{-/-}$ mice as compared with that in *CD47*$^{+/+}$ mice ($p < 0.01$; Fig. 9, *A* and *B*). In 28-week-old *CD47*$^{-/-}$ mice, the trabecular bone volume was further reduced to 45% of that in *CD47*$^{+/+}$ mice ($p < 0.001$; Fig. 9*B*). These differences in trabecular bone microarchitecture were also confirmed by micro-computed tomography (Fig. 9*C*). To further investigate this intriguing observation, we next examined bone formation in 18-week-old *CD47*$^{+/+}$ or *CD47*$^{-/-}$ mice using dual calcein labeling *in vivo* (Fig. 9*D*). These experiments revealed that the bone formation rate was markedly reduced in 18-week-old *CD47*$^{-/-}$ mice, being 62% of that in *CD47*$^{+/+}$ mice (0.26 ± 0.008 $\mu m^2/\mu m^3$/day *versus* 0.10 ± 0.030 $\mu m^2/\mu m^3$/day, $p < 0.001$; Fig. 9*D*). This inhibition was consistent with a reduction of both osteoblast activity and surface extent, with mineral apposition rate and mineralizing surface reduced by 34 and 42%, respectively ($p < 0.01$; Fig. 9*D*). In 28-week-old *CD47*$^{+/+}$ mice, the mineralized surface, mineral apposition rate, and bone formation rate were much lower, as compared with that in 18-week-old *CD47*$^{+/+}$ mice (Fig. 9*D*), and no difference in these parameters were seen between *CD47*$^{+/+}$ or *CD47*$^{-/-}$ mice at 28 weeks of age (Fig. 9*D*). In line with the reduced mineralization observed in 18-week-old *CD47*$^{-/-}$ mice, these mice were also found to have a 66% reduction in osteoid surface, as compared with that in age-matched *CD47*$^{+/+}$ mice ($p < 0.001$; Fig. 9*D*). In 28-week-old *CD47*$^{-/-}$ mice, osteoid surface was reduced by 43%, as compared with that in *CD47*$^{+/+}$ mice (Fig. 9*D*).

We also investigated the cortical bone compartment in 18- or 28-week-old *CD47*$^{+/+}$ and *CD47*$^{-/-}$ mice, using peripheral

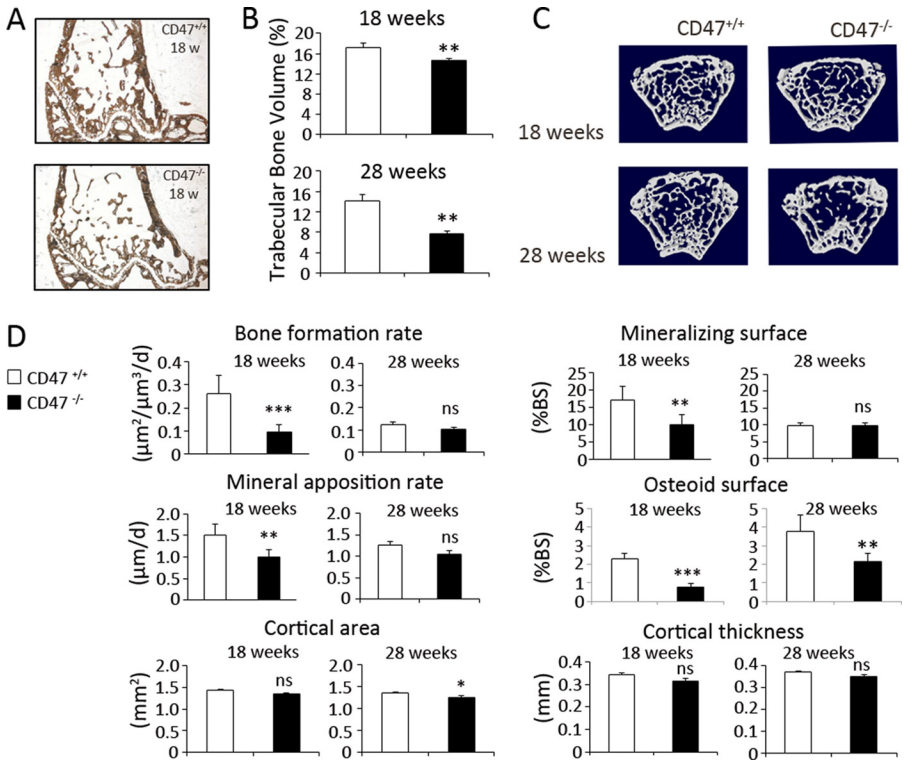

FIGURE 9. **Reduced bone formation in *CD47*$^{-/-}$ mice.** *A*, representative femoral sections from 18-week-old *CD47*$^{+/+}$ and *CD47*$^{-/-}$ mice stained for mineral with von Kossa. *B*, at 18 and 28 weeks of age, the trabecular bone volume was lower in *CD47*$^{-/-}$ mice, as compared with age-matched *CD47*$^{+/+}$ mice. *C*, micro-computed tomography images of left femur from 18- and 28-week-old *CD47*$^{+/+}$ and *CD47*$^{-/-}$ mice. At 18 weeks of age, trabecular bone formation rate, mineral apposition rate, and mineralizing surface were all significantly reduced in femurs from *CD47*$^{-/-}$ mice, as compared with that in *CD47*$^{+/+}$ mice. At 28 weeks of age, the same parameters did not show any significant differences between *CD47*$^{+/+}$ and *CD47*$^{-/-}$ mice. Osteoid surface was significantly lower in *CD47*$^{-/-}$ mice at both 18 and 28 weeks, as compared with that in *CD47*$^{+/+}$ mice. A non-significant (*ns*) difference was seen in cortical area, when comparing *CD47*$^{+/+}$ and *CD47*$^{-/-}$ mice at 18 weeks of age; however, a 6% statistically significant difference was evident in cortical area at 28 weeks of age. The cortical thickness was not significantly different in the two genotypes at 18 or 28 weeks of age. Data are means ± S.E. of 7–10 mice in each age group. *ns*, not significant. *, $p < 0.05$; **, $p < 0.01$; and ***, $p < 0.001$, as compared with that in *CD47*$^{+/+}$ mice, using Student's *t* test for unpaired analyses. *d*, day.

quantitative computed tomography analysis. Although this analysis showed a slight decrease in cortical area and thickness in both 18- and 28-week-old *CD47*$^{-/-}$ mice, the only statistically significant difference was detected in cortical area of 28-week-old *CD47*$^{-/-}$ mice (Fig. 9*D*). Note that there were no differences in bone marrow fat content in 28-week-old *CD47*$^{+/+}$ and *CD47*$^{-/-}$ mice (data not shown).

DISCUSSION

The mechanisms regulating bone homeostasis are multiple and still not fully understood. In the present study, we have shown that CD47 is required to activate its receptor SIRPα in stromal cells/osteoblasts, which is critically important within the bone marrow for the ability of stromal cells/osteoblasts to promote formation of osteoclasts. Lack of CD47/SIRPα signaling in the stromal cell compartment impairs osteoblast differentiation *in vivo* and *in vitro*. This functional defect not only impairs osteoid formation and mineralization *in vivo* but also results in impaired formation of osteoclasts. Together, this suggests an explanation to the osteopenic bone phenotype of *CD47*$^{-/-}$ mice.

Investigations of osteoclast formation *in vitro* are based on a number of different experimental systems, which show important variations. One system is based on selection of monocyte/macrophage progenitors from the bone marrow and differentiation of these cells toward the osteoclastic lineage by addition of M-CSF and RANKL to the culture medium (bone marrow myeloid precursor cell (BMM) cultures) (21). Another system can be used to mimic more physiological conditions *in vivo*, which is based on the culture of crude bone marrow (BMC cultures), containing both stromal cells (with osteoblast progenitor potential) and hematopoietic progenitor cells (which can differentiate into pre-osteoclasts) (22). In the latter system, which is used in this paper, stimulation with PTH or D3 will induce stromal cells/osteoblasts to produce RANKL, resulting in a natural indirect stimulation of pre-osteoclast differentiation and osteoclast maturation. The importance of stromal cells can be bypassed if M-CSF and RANKL are added to this type of culture.

Our previous data suggest that the physical interaction between CD47 and SIRPα is important for osteoclast formation in BMM cultures because functional blocking antibodies against either CD47 or SIRPα impaired osteoclast formation in *CD47*$^{+/+}$ cultures, and that *CD47*$^{-/-}$ BMM cultures generated less osteoclasts than *CD47*$^{+/+}$ cultures (12). Uluçkan *et al.* (13) also showed impaired generation of osteoclasts from *CD47*$^{-/-}$ BMM cells but that the osteoclast formation defect could be rescued by pre-incubation with M-CSF and by increasing the levels of RANKL. We have confirmed the rescued osteoclast formation in *CD47*$^{-/-}$ BMM cultures by pre-incubating the cells with M-CSF and by adding increased concentrations of

RANKL or a highly efficient truncated form of RANKL (data not shown). This is an interesting observation, suggesting that M-CSF-mediated early differentiation of pre-osteoclasts can rescue the osteoclast phenotype in *CD47*$^{-/-}$ mice if sufficient RANKL levels are provided.

In the present study, we found that osteoclast formation was virtually abolished in *CD47*$^{-/-}$ BMC stimulated with PTH or D3 *in vitro*. In this more complex system, the observed defect cannot only be explained as a pre-osteoclast fusion defect, since gene expression levels of *nfatc1*, *oscar*, *Trap/Acp5*, the *ctr*, and *catK*, all important markers of differentiation along the osteoclastic lineage (5, 23), were strongly impaired as well, whereas the expression levels of the M-CSF receptor *c-fms* or that of *SIRPα* were not impaired in *CD47*$^{-/-}$ BMC. Rather, our data suggest that a key defect in *CD47*$^{-/-}$ BMC is associated with impaired function and differentiation of stromal cells along the osteoblastic lineage. These cells, when stimulated with PTH or D3, are induced to produce M-CSF and RANKL, which are pivotal to drive osteoclast differentiation and formation in this system and also *in vivo* (4). It is therefore interesting to note that D3-stimulated M-CSF and RANKL expression in *CD47*$^{-/-}$ BMC were both strongly reduced at the gene as well as protein levels and that these cultures showed a very low TRAP activity. The importance of this finding is emphasized by data from Maile *et al.* (14), showing that addition of exogenous M-CSF and RANKL to a crude *CD47*$^{-/-}$ bone marrow cultures rendered the same TRAP staining levels as in *CD47*$^{+/+}$ cultures.

The lack of M-CSF and RANKL expression in *CD47*$^{-/-}$ BMC pointed toward a phenotypic change in the bone marrow stromal cells when CD47 was absent. To further understand the mechanism behind this, we investigated the hypothesis that the stromal cell defect was due to the absence of CD47-mediated induction of SIRPα signaling. We found a strongly decreased tyrosine phosphorylation of SIRPα in bone marrow stromal cells when CD47 was absent. Together with the results from the co-culture experiments, showing that bone marrow stromal cells lacking either CD47 or the signaling domain of SIRPα could not efficiently support osteoclast formation, this clearly suggests that SIRPα signaling in bone marrow stromal cells is necessary for osteoclastogenesis. The fact that osteoclast formation was intact in bone marrow macrophages, lacking either CD47 or the SIRPα signaling domain, when cultured on wild-type bone marrow stromal cells, further suggest that the impaired osteoclast formation in *CD47*$^{-/-}$ BMC cultures was unlikely due to lack of CD47/SIRPα interaction in pre-osteoclasts but that the defect was rather isolated to the stromal cells.

In 2011, Maile *et al.* (14) showed an impaired osteoclast formation in *CD47*$^{-/-}$ crude bone marrow cells cultured in the presence of M-CSF and RANKL. The authors suggested that the physical interaction between CD47 and SIRPα induced SIRPα tyrosine phosphorylation, recruitment of SHP-1, and subsequent dephosphorylation of non-muscle cell myosin IIA, which, altogether, would be important to promote fusion and formation of osteoclasts (14). It is hard to interpret these data because the osteoclast formation was driven by addition of exogenous M-CSF and RANKL to the crude bone marrow culture, which based on data from the present study and that of a previous study (13) can compensate for the lack of CD47. The reason why Maile *et al.* (14) only detected late fusion defects when CD47 was missing in the cultures could be that the early osteoclast precursors proliferated and differentiated in the presence of M-CSF. In marked contrast, data by van Beek *et al.* (24) in 2009 showed that bone marrow cells from SIRPα mutant mice (lacking the signaling SIRPα cytoplasmic domain, but expressing the extracellular CD47-binding domain of SIRPα) generated normal numbers of osteoclasts with the same number of nuclei, as compared with that in wild-type bone marrow cultures, when cultured with exogenous M-CSF and RANKL (24). Notably, van Beek *et al.* (24) used a truncated form of mouse RANKL with a much lower EC_{50} value then the human RANKL that was used by Maile *et al.* (14), which could be one explanation behind the normal osteoclast formation in SIRPα mutant bone marrow cultures.

The stromal cell phenotypic change apparent when CD47 was missing did not only impair osteoclast differentiation but also affected the osteoblast differentiation pathway. At the gene expression level, we found an impaired expression of *runx2* and α-1-collagen and a virtually blunted expression of osterix and *Alp*/*Akp1*, whereas the expression of the adipocyte-associated gene *PPARγ2* was found to be normal. To find out whether the mechanism of action in *CD47*$^{-/-}$ cells was lack of SIRPα signaling, we took advantage of the SIRPα mutant mice where the cytoplasmic SIRPα domain is deleted and cannot be phosphorylated. Culture of bone marrow stromal cells from these mice showed dramatically decreased alkaline phosphatase activity. These findings support the hypothesis that CD47 has a profound effect on osteoblastic differentiation by inducing activation of SIRPα signaling. Further studies of the downstream signaling from SIRPα in stromal cells are necessary to understand how the receptor is linked to the master regulator of osteoblast differentiation, RUNX-2.

The strong *in vitro* phenotype in *CD47*$^{-/-}$ BMC suggested that there should also be an obvious bone phenotype in these mice *in vivo*. We previously reported that 18-week-old *CD47*$^{-/-}$ mice had reduced numbers of osteoclasts *in vivo* (12), which we in the present study confirmed to also be the case in 28-weeks old *CD47*$^{-/-}$ mice. By looking at the osteoclast phenotype *per se*, one would assume that *CD47*$^{-/-}$ mice would present with an osteopetrotic bone phenotype. However, in agreement with the data from our *in vitro* BMC experiments, analyses of the skeleton in 18-week-old *CD47*$^{-/-}$ mice indeed demonstrate an osteopenic bone phenotype including a reduced trabecular bone volume, bone mineral density, bone formation rate, mineral apposition rate, and osteoblast number. Furthermore, aged 28-week-old *CD47*$^{-/-}$ mice showed a persistent osteopenic bone phenotype with reduced numbers of osteoblasts and osteoclasts. Our bone phenotype data in *CD47*$^{-/-}$ mice, on the Balb/c background, are in part confirmed by data from C57BL/6 *CD47*$^{-/-}$ mice where an osteopenic bone phenotype was demonstrated (14). Although lack of CD47 was not associated with a reduced number of osteoclasts in the bones of C57BL/6 mice, which could possibly be explained by strain differences (13, 14). Van Beek *et al.* (24) showed that the SIRPα mutant mice had a decreased cortical bone volume, suggested to be due to an increased bone resorbing activity of osteoclasts lacking SIRPα.

In conclusion, in a physiologically relevant *in vitro* system where stromal cells/osteoblasts regulate differentiation and formation of osteoclasts, lack of CD47 or the signaling domain of SIRPα in stromal cells results in a dramatically impaired osteoclast formation. These findings identify a mechanism where CD47 induces tyrosine phosphorylation of SIRPα in bone marrow stromal cells, which appears to be pivotal for normal osteoblast differentiation and ability to stimulate osteoclast formation. The biological importance of this mechanism is also confirmed by the osteopenic bone phenotype in *CD47*$^{-/-}$ mice.

Acknowledgments—We thank Anita Lie, Rima Sulniute, and Barbro Borgström for skillful technical support and are grateful to Professor Ulf Lerner for critically reading and commenting on the manuscript.

REFERENCES

1. Nakashima, T., Hayashi, M., Fukunaga, T., Kurata, K., Oh-Hora, M., Feng, J. Q., Bonewald, L. F., Kodama, T., Wutz, A., Wagner, E. F., Penninger, J. M., and Takayanagi, H. (2011) Evidence for osteocyte regulation of bone homeostasis through RANKL expression. *Nat. Med.* **17,** 1231–1234
2. Xiong, J., Onal, M., Jilka, R. L., Weinstein, R. S., Manolagas, S. C., and O'Brien, C. A. (2011) Matrix-embedded cells control osteoclast formation. *Nat. Med.* **17,** 1235–1241
3. Yoshida, H., Hayashi, S., Kunisada, T., Ogawa, M., Nishikawa, S., Okamura, H., Sudo, T., Shultz, L. D., and Nishikawa, S. (1990) The murine mutation osteopetrosis is in the coding region of the macrophage colony stimulating factor gene. *Nature* **345,** 442–444
4. Teitelbaum, S. L., and Ross, F. P. (2003) Genetic regulation of osteoclast development and function. *Nat. Rev. Genet.* **4,** 638–649
5. Boyle, W. J., Simonet, W. S., and Lacey, D. L. (2003) Osteoclast differentiation and activation. *Nature* **423,** 337–342
6. Stein, G. S., and Lian, J. B. (1993) Molecular mechanisms mediating proliferation/differentiation interrelationships during progressive development of the osteoblast phenotype. *Endocr. Rev.* **14,** 424–442
7. Stein, G. S., Lian, J. B., and Owen, T. A. (1990) Relationship of cell growth to the regulation of tissue-specific gene expression during osteoblast differentiation. *FASEB J.* **4,** 3111–3123
8. Kukreja, A., Radfar, S., Sun, B. H., Insogna, K., and Dhodapkar, M. V. (2009) Dominant role of CD47-thrombospondin-1 interactions in myeloma-induced fusion of human dendritic cells: implications for bone disease. *Blood* **114,** 3413–3421
9. Brown, E. J., and Frazier, W. A. (2001) Integrin-associated protein (CD47) and its ligands. *Trends Cell Biol.* **11,** 130–135
10. Han, X., Sterling, H., Chen, Y., Saginario, C., Brown, E. J., Frazier, W. A., Lindberg, F. P., and Vignery, A. (2000) CD47, a ligand for the macrophage fusion receptor, participates in macrophage multinucleation. *J. Biol. Chem.* **275,** 37984–37992
11. Vignery, A. (2000) Osteoclasts and giant cells: macrophage-macrophage fusion mechanism. *Int. J. Exp. Pathol.* **81,** 291–304
12. Lundberg, P., Koskinen, C., Baldock, P. A., Löthgren, H., Stenberg, A., Lerner, U. H., and Oldenborg, P. A. (2007) Osteoclast formation is strongly reduced both *in vivo* and *in vitro* in the absence of CD47/SIRPα-interaction. *Biochem. Biophys. Res. Commun.* **352,** 444–448
13. Uluçkan, O., Becker, S. N., Deng, H., Zou, W., Prior, J. L., Piwnica-Worms, D., Frazier, W. A., and Weilbaecher, K. N. (2009) CD47 regulates bone mass and tumor metastasis to bone. *Cancer Res.* **69,** 3196–3204
14. Maile, L. A., DeMambro, V. E., Wai, C., Lotinun, S., Aday, A. W., Capps, B. E., Beamer, W. G., Rosen, C. J., and Clemmons, D. R. (2011) An essential role for the association of CD47 to SHPS-1 in skeletal remodeling. *J. Bone Miner. Res.* **26,** 2068–2081
15. Lindberg, F. P., Bullard, D. C., Caver, T. E., Gresham, H. D., Beaudet, A. L., and Brown, E. J. (1996) Decreased resistance to bacterial infection and granulocyte defects in IAP-deficient mice. *Science* **274,** 795–798
16. Inagaki, K., Yamao, T., Noguchi, T., Matozaki, T., Fukunaga, K., Takada, T., Hosooka, T., Akira, S., and Kasuga, M. (2000) SHPS-1 regulates integrin-mediated cytoskeletal reorganization and cell motility. *EMBO J.* **19,** 6721–6731
17. Okazawa, H., Motegi, S., Ohyama, N., Ohnishi, H., Tomizawa, T., Kaneko, Y., Oldenborg, P. A., Ishikawa, O., and Matozaki, T. (2005) Negative regulation of phagocytosis in macrophages by the CD47-SHPS-1 system. *J. Immunol.* **174,** 2004–2011
18. Baldock, P. A., Sainsbury, A., Allison, S., Lin, E. J., Couzens, M., Boey, D., Enriquez, R., During, M., Herzog, H., and Gardiner, E. M. (2005) Hypothalamic control of bone formation: distinct actions of leptin and y2 receptor pathways. *J. Bone Miner Res.* **20,** 1851–1857
19. Nishimura, R., Hata, K., Ikeda, F., Ichida, F., Shimoyama, A., Matsubara, T., Wada, M., Amano, K., and Yoneda, T. (2008) Signal transduction and transcriptional regulation during mesenchymal cell differentiation. *J. Bone Miner. Metab.* **26,** 203–212
20. Johansen, M. L., and Brown, E. J. (2007) Dual regulation of SIRPα phosphorylation by integrins and CD47. *J. Biol. Chem.* **282,** 24219–24230
21. Takeshita, S., Kaji, K., and Kudo, A. (2000) Identification and characterization of the new osteoclast progenitor with macrophage phenotypes being able to differentiate into mature osteoclasts. *J. Bone Miner. Res.* **15,** 1477–1488
22. Conaway, H. H., Persson, E., Halén, M., Granholm, S., Svensson, O., Pettersson, U., Lie, A., and Lerner, U. H. (2009) Retinoids inhibit differentiation of hematopoietic osteoclast progenitors. *FASEB J.* **23,** 3526–3538
23. Nemeth, K., Schoppet, M., Al-Fakhri, N., Helas, S., Jessberger, R., Hofbauer, L. C., and Goettsch, C. (2011) The role of osteoclast-associated receptor in osteoimmunology. *J. Immunol.* **186,** 13–18
24. van Beek, E. M., de Vries, T. J., Mulder, L., Schoenmaker, T., Hoeben, K. A., Matozaki, T., Langenbach, G. E., Kraal, G., Everts, V., and van den Berg, T. K. (2009) Inhibitory regulation of osteoclast bone resorption by signal regulatory protein α. *FASEB J.***23,** 4081–4090